

Efficient Bi-doped fiber lasers and amplifiers for the spectral region 1300-1500 nm

I.A. Bufetov^a, M.A. Melkumov^{*a}, V.F. Khopin^b, S.V. Firstov^a, A.V. Shubin^a, O.I. Medvedkov^a,
A.N. Guryanov^b, E.M. Dianov^a

^a Fiber Optics Research Center of the Russian Academy of Sciences, 38 Vavilov Str., Moscow,
Russia 119333

^b Institute of Chemistry of High Purity Substances of the Russian Academy of Sciences, 49 Tropinin
Str., N.Novgorod, Russia 603950

ABSTRACT

Watt-level Bi fiber lasers have been demonstrated at 1280, 1330, 1340, 1360 and 1480 nm with the maximum output power of up to 10W and with the efficiency of up to 50% for the first time. The bismuth-doped phosphogermanosilicate fiber amplifiers operating within the wavelength range 1300-1500 nm have been developed. The net gain of more than 20 dB at the wavelengths of 1320 and 1440 nm under the 200-300 mW pump power was obtained. The 3 dB bandwidth of the amplifiers was larger than 30 nm, the noise figure being 4-6 dB.

Keywords: fiber lasers, fiber amplifiers, bismuth-doped fibers, bismuth fiber lasers, fiber-optics.

1. INTRODUCTION

Bismuth-doped fibers are a new type of laser active medium demonstrating optical gain within a wavelength range of 1150-1550 nm (see review [1] and references therein). Near-IR luminescence in Bi-doped silica glass was discovered ten years ago, in 1999 [2]. Since that time, the near-IR luminescence has been observed and investigated in many Bi-doped glasses of various compositions, the first Bi-doped fibers have been developed [3, 4] and a family of Bi-doped fiber lasers has been demonstrated [1]. These lasers were based on Bi-doped aluminosilicate fibers (ASB fibers) and operate within a wavelength range of 1140-1215 nm. The variation of the fiber core composition enabled one to obtain luminescence and lasing in the wavelength band of 1300-1550 nm with an efficiency of 1-5% [5, 6]. These results were obtained using Bi-doped phosphogermanosilicate fibers (PGSB fibers). In a number of papers optical gain properties of Bi-doped glasses [7, 8] and fibers [3, 9] were investigated. The maximal gain achieved was ≈ 13 dB at the wavelength of 1440 nm under pump power of 1W [10].

In this paper, we used PGSB fibers to obtain lasers and amplifiers in the wavelength region 1300-1500 nm with a higher output power and higher efficiency of lasers and with a higher gain and gain coefficient of amplifiers. We investigated the characteristics of a number of lasers operating in the wavelength range 1280-1480 nm. We studied the properties of optical amplifiers operating in the wavelength ranges near 1320 and 1440 nm.

2. BI-DOPED FIBERS

We fabricated preforms for PGSB fibers by the MCVD technique. The fiber core glass with all dopants was deposited from the vapor phase. For Bi-doped fiber lasers and amplifiers we used here two types of PGSB fibers: F1 and F2. The maximal index difference between the core and the cladding for F1 was $\Delta n = 8.5 \cdot 10^{-3}$, the mode field diameter at the wavelength $\lambda = 1300$ nm MFD = 6.4 μm , the cutoff wavelength $\lambda_c = 1200$ nm. For F2, these values were $\Delta n = 22 \cdot 10^{-3}$, MFD = 4.1 μm , and $\lambda_c = 1200$ nm. The bismuth concentration in the core of F1 and F2 was less than 0.02 at.% (the sensitivity limit of our equipment). Fig. 1 and Fig. 2 shows the loss and excitation spectra of these fibers. The data from these graphs were used to estimate the necessary lengths of fibers and pump wavelengths for Bi-doped fiber lasers and amplifiers (BDFAs). Preliminary results concerning BDFAs at 1320 nm were published in [11].

*melkumov@fo.gpi.ru; phone 7(499)5038121; fax 7(499)1358139

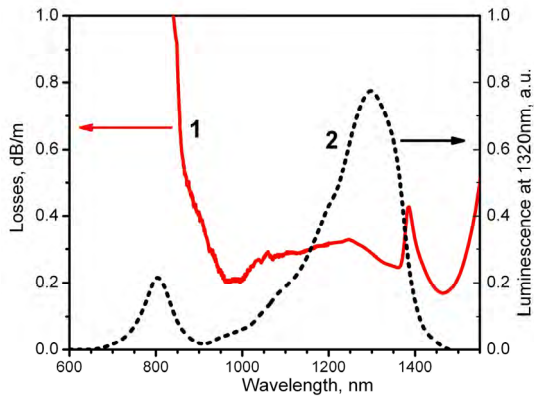


Fig. 1. F1 fiber: optical loss spectrum (1) and excitation spectrum of 1320 nm luminescence (2).

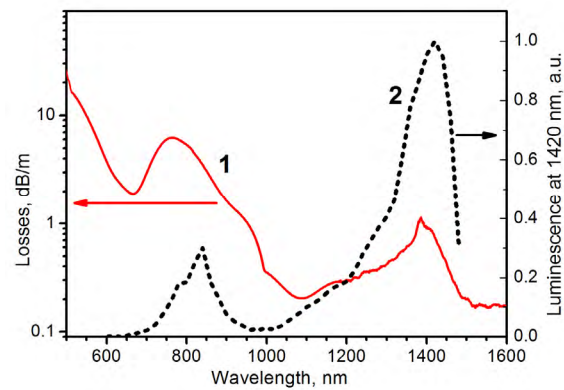


Fig. 2. F2 fiber: optical loss spectrum (1) and excitation spectrum of 1440 nm luminescence (2).

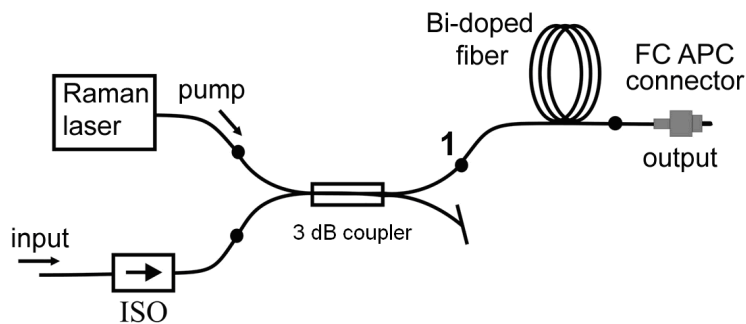


Fig. 3. The schematic of the BDFA. 1- splicing points.

3. BI-DOPED FIBER AMPLIFIERS FOR THE WAVELENGTH REGION 1300-1500 NM

Bismuth-doped fibers F1 and F2 were tested as gain media in the fiber amplifiers. Two cw Raman fiber lasers at 1230 nm and 1318 nm with a 1.5 W output power were used as pump sources for these amplifiers. The amplifier schematic is presented in Fig. 3. The active fiber length of bismuth-doped fiber was ~200 m in both cases.

We used three fiber-coupled sources as a signal: wideband (1250-1550 nm) super-luminescent diodes, a narrowband Raman fiber laser at 1318 nm, and a FBG stabilized laser diode at 1433 nm. The wideband source was used for measurements of the spectral characteristics of the amplifiers. The narrowband sources were utilized for the investigations of the saturation characteristics of the bismuth-doped fibers. We launched the signal through the isolator (ISO in Fig. 3). A 3 dB coupler was used to launch the radiation of the pump and the signal into the active fiber. A bare end of the coupler was used to control the pump and the signal power. After all measurements, we cut almost all active fiber and recorded output power and spectra of the pump and the signal in the Bi-doped fiber just 10-15 cm after the input splice. To reduce the back reflection from the fiber endface we spliced the output end of the bismuth-doped fiber with the FC APC connector (the angle polished FC connector). The output spectra and the power were registered with the aid of optical spectrum analyzer Agilent 86140B and optical power meter Ophir Nova II.

Net gain (G) and noise figure (NF) spectra of the F1 and F2 based fiber amplifiers at a pump power level of 460 mW (F1) and 190 mW (F2) are presented in Fig. 4 a) and b), respectively. The noise figure was calculated according to [12]

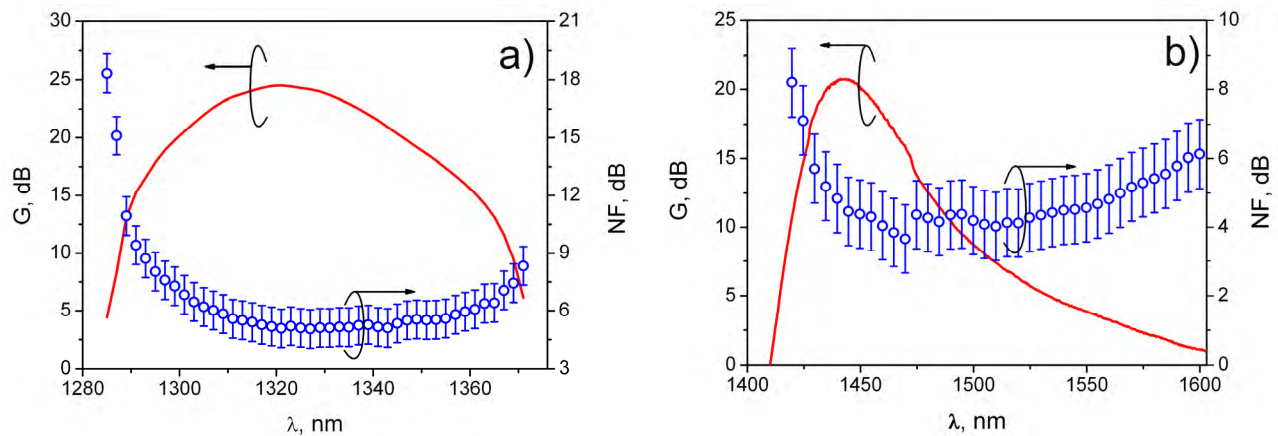


Fig. 4. Net gain (left scale) and noise figure (right scale) of the F1 (a) and F2 (b) fibers.

using the measured ASE power and the net gain. The noise figure defines the noise characteristics of the amplifier and equals the ratio of OSNR at the amplifier input to that at amplifier output. The minimal NF of our amplifiers was 4-6 dB.

The net gain was positive in the wavelength range 1283-1372 nm for F1 and 1410-1600 for F2. The gain maximum was near 1321 nm and 1442 nm in F1 and F2, respectively, reaching 24,5 dB (F1) and 20.7 dB (F2). The 3 dB bandwidth of the net gain was 37 nm in F1 and 34 nm in F2.

Fig. 5 shows the dependencies of the small signal gain for F1 at 1318 nm (Fig. 5 a) and for F2 at 1433 nm (Fig. 5 b) vs. the launched pump power - P_{pump} . The maximum gain efficiency achieved G_{max} is defined as a slope of the dashed straight line going through the zero point. It is equal to ~ 0.09 dB/mW and $0,22$ dB/mW for F1 and F2, respectively.

The dependences of the net gain at 1318 nm (F1) and 1433 nm (F2) on the signal power are shown in Fig. 6 a) and b).

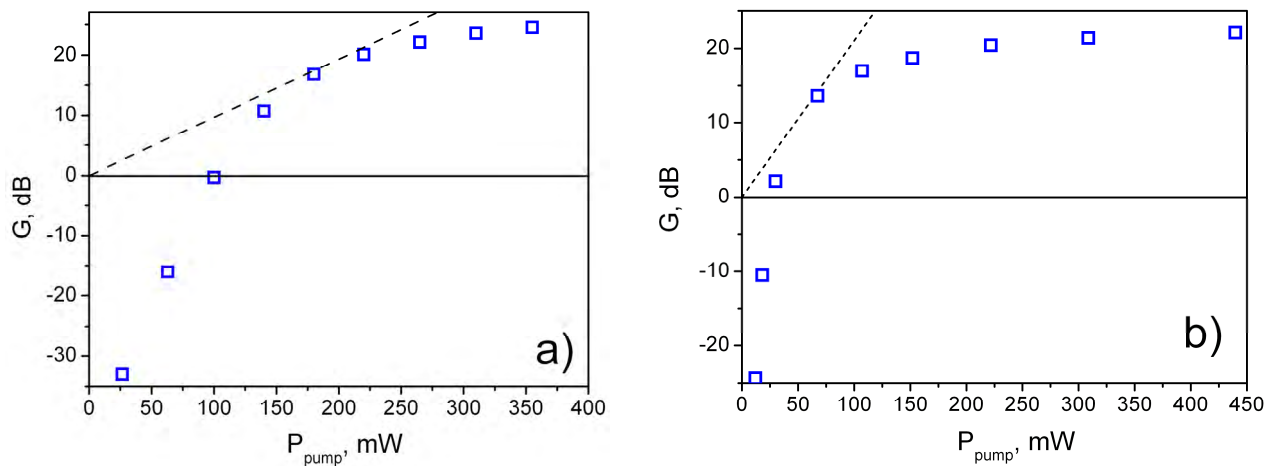


Fig. 5. Dependence of the net gain on the launched pump power for F1 (a) and F2 (b).

The pump power was 350 mW and 460 mW for F1 and 235 mW and 450 mW for F2. The signal saturation power P_{sat} in fiber F1 was equal to 9.5 dBm (10,5 dBm) for pump power 350 mW (460 mW). In fiber F2 it was 6.5 dBm (9,9 dBm) for pump power 235 mW (450 mW).

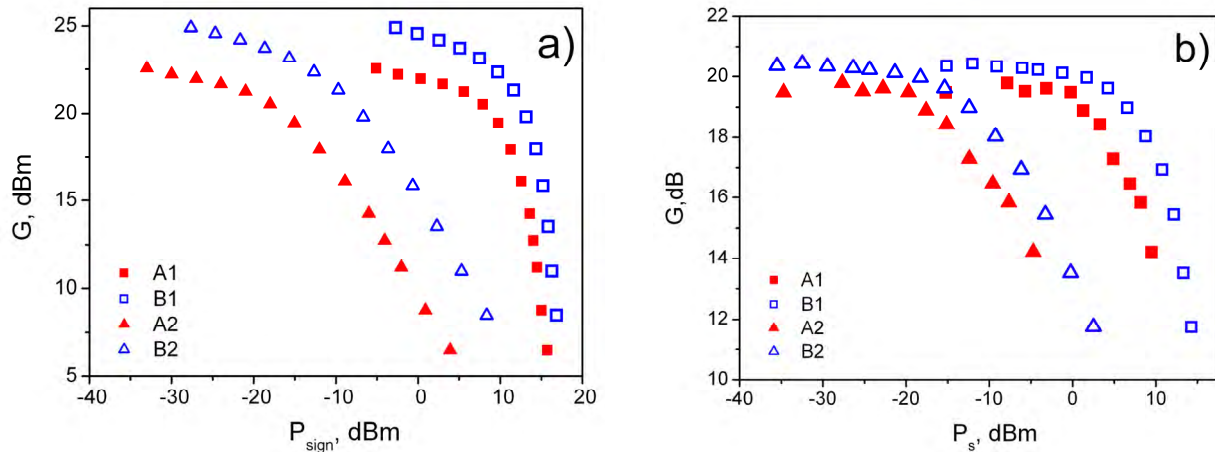


Fig. 6. Dependences of the net gain G on the signal power P_{sign} in F1 (a) and F2 (b). Squares and triangles represent the dependencies on signal power at the output end and at the input of the amplifier, respectively. Letters “A” and “B” represent dependencies for different pump powers: a) A1 and A2: $P_{\text{pump}}=350$ mW, B1 and B2: $P_{\text{pump}}=460$ mW, b) A1 and A2: $P_{\text{pump}}=235$ mW, B1 and B2: $P_{\text{pump}}=450$ mW.

The power conversion efficiency in the saturated regime normalized to the launched pump power reached $\sim 9\%$ in F1 and $\sim 6.3\%$ in F2 while the net gain was equal to 10 dB. We believe that such a low efficiency was due to noticeable value of background loss in the bismuth-doped fibers and probably due to influence of ESA, which taken together provide unbleachable losses of the order of 30 dB/km.

4. SCHEME OF CW BISMUTH FIBER LASERS

The measured gain spectra of the F1 and F2 fibers show the possibility to design fiber lasers at the wavelengths in the range of these gain spectra (see Fig. 7). We developed a set of bismuth lasers with a relatively high optical-to-optical efficiency at the wavelength from 1280 to 1480 nm. One and the same scheme shown in Fig. 8 was used for all these lasers. As an active medium for lasers in the 1280-1360 nm band, the F1 fiber was used, and for lasers at 1480 nm the F2 fiber was applied. Index Bragg gratings (BG) written in the core of special lengths of fibers were used as mirrors of the laser cavity. The resonance wavelengths of these BGs defined the laser wavelength of each laser. The reflection

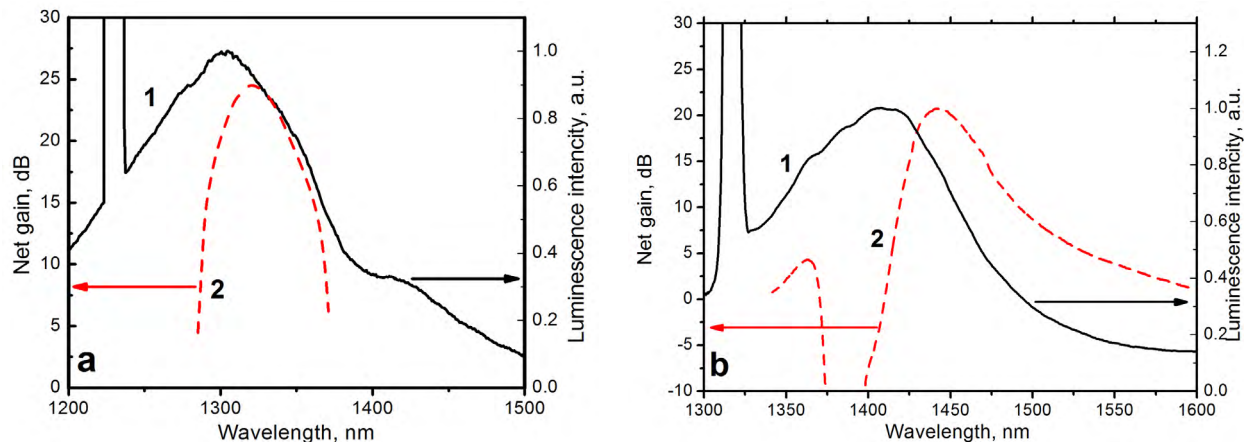


Fig. 7. Luminescence and net gain spectra of the F1 (a) and F2 (b) fibers pumped at 1230 nm and 1318 nm, respectively.

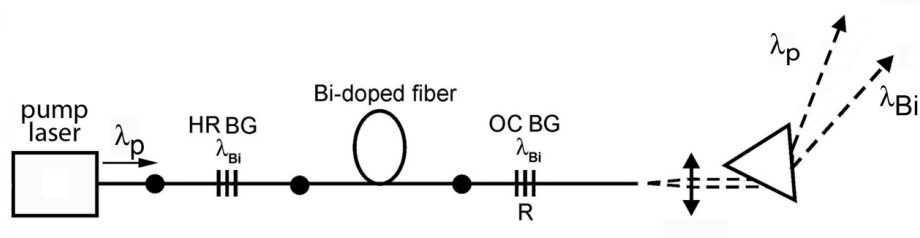


Fig. 8. The scheme of the cw single mode Bi-doped fiber laser.

bandwidth of BGs was approximately 0.5 nm. One of BGs in each laser cavity had a reflectivity close to 100% (HR BG). The output BG (OC BG) had a reflectivity in the range 3.5-50% for various lasers. As a pump sources for single-mode Bi-doped lasers we used single-mode Raman lasers at the wavelength of 1230 nm (for bismuth lasers at 1280-1360 nm) and 1340 nm (for lasers at 1480 nm). The maximal available output power of the fiber Raman laser at 1230 nm was 30 W, and the available power at 1318 nm was 10W. The length of the active fibers for lasers were determined as 100 m for the F1 fiber and 90 m for the F2 fiber.

5. OUTPUT LASER PARAMETERS

5.1 Lasers at wavelength in the vicinity of 1300 nm.

The Bi-doped fiber lasers (BFLs) based on the F1 fiber operating at the wavelengths of 1280, 1330, 1340, and 1360 nm were investigated. At each wavelength BFLs with different OC BGs were compared. Fig. 9 shows the dependences of the laser radiation output power on the absorbed pump power for nine BFLs at wavelengths indicated above. Some of the output parameters of these lasers are shown in Table 1, where:

R_{OC} is the reflectivity of the OC BG,

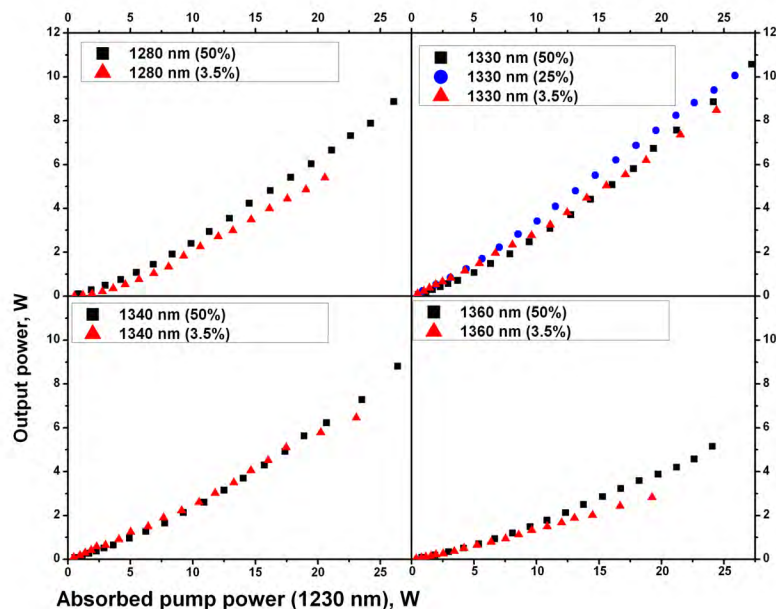


Fig. 9 Variation of the output power with the absorbed pump power for Bi-fiber lasers at different lasing wavelengths. The lasing wavelength and the OC reflectivity are indicated in each graph.

λ_L is the laser wavelength,

P_{out}^{max} is the maximal output laser power observed,

P_{pl} is the pump power launched into the Bi-doped fiber,

P_{pl}^{max} is the maximal pump power launched into the Bi-doped fiber,

$\eta(P_{pl}^{max})$ is the laser efficiency with respect to the pump power launched into the fiber at the maximal launched pump power available in our experiment,

η_s^{max} is the maximal slope efficiency of the laser with respect to P_{pl}

η_{s0} is the slope efficiency of the Bi laser at low values of the pump power (with respect to P_{pl}).

Table 1. Parameters of PGSB fiber lasers

| Laser designation $L(\lambda_L(\text{nm}), R_{oc}(\%))$ | P_{out}^{max} , W | $\eta(P_{pl}^{max})$, % | η_s^{max} , % | η_{s0} , % |
|--|---------------------|--------------------------|--------------------|-----------------|
| L(1280, 50) | 8.9 | 31 (28.3 W) | 40 | 14 |
| L(1280, 3.5) | 5.4 | 19 (28.3 W) | 27 | 3 |
| L(1330, 50) | 10.6 | 37 (28.8 W) | 50 | 17 |
| L(1330, 25) | 10.06 | 36 (28.3 W) | 40 | 22 |
| L(1330, 3.5) | 8.5 | 29 (28.8W) | 36 | 19 |
| L(1340, 50) | 8.8 | 31 (28.8 W) | 40 | 15 |
| L(1340, 3.5) | 6.5 | 23 (28.8 W) | 2.6 | 13 |
| L(1360, 50) | 5.23 | 18 (28.8 W) | 23 | 9.5 |
| L(1360, 3.5) | 2.8 | 9.8 (28.8 W) | 12 | 7.1 |
| L(1480, 50) | 1.94 | 21 (9.3 W) | 25 | 9.1 |
| L(1480, 3.5) | 0.95 | 13.3 (7.1 W) | 18 | - |

It is worth noting that presentation of the output parameters of a laser as functions on the absorbed pump power (as in Fig. 9) is most informative from the scientific point of view. However, the data with respect to the pump power launched

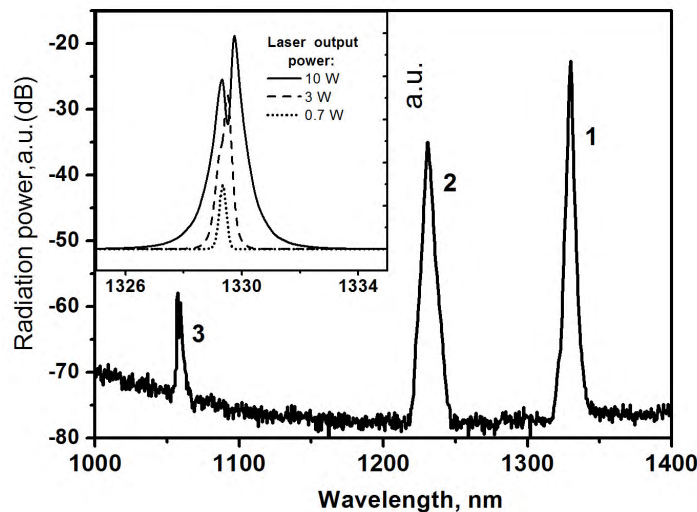


Fig. 10. Output spectrum of the Bi-fiber laser, $P_{pl}=28\text{W}$. 1 - Bi laser output radiation; 2 - unabsorbed pump radiation; 3 – residual pump for Raman laser (Yb-fiber laser radiation). The inset shows the spectrum of the output radiation of the BFL for various output powers (on a linear scale).

into the active fiber (as in Table 1) are of interest for practical applications.

The threshold pump powers for all lasers are of the order of 100 mW. The peculiarity of dependences shown in Fig. 9 is clearly visible nonlinearity. The slope efficiency for all curves is lower at small pump powers (compare with the data in Table 1), and we observe an increase of the slope efficiency with an increase of pump power. And the degree of nonlinearity depends on the reflectivity of the OC BG and on the laser wavelength. The most linear dependence of the laser output power on the pump power is observed for laser L(1330, 25) (Table 1).

The reflectivity of the OC BG affects the efficiency of the laser, and, consequently, there exists a problem of OC BG optimization. As one would expect, the maximal Bi-laser efficiency is observed for a laser generating at the wavelength near the maximum of the optical fiber gain (1330 nm). The maximal value of the slope efficiency reaches 50% for laser L(1330, 50) (Table 1). At the same time, the total optical efficiency of this laser (with respect to the pump power launched into the fiber) is 35%. Laser L(1330, 50) demonstrated the maximal obtained output power of 10.6 W at the pump power of 28.8 W.

The typical radiation spectrum at the output of the Bi-fiber laser is shown in Fig. 10. One can see that at the output of the Bi-fiber laser there is a negligible part of the pump radiation for the Raman laser ($\lambda=1058$ nm). The unabsorbed pump radiation power ($\lambda=1230$ nm) is approximately an order of magnitude lower than the output power of the BFL. The variation of the spectrum of the output radiation with the output power (see inset in Fig. 10) indicates broadening of the output spectrum with increasing power. The local minimum at the output spectrum (10 W output power, Fig. 10, inset) reveals the variation of the effective reflectivity of the OC BG due to broadening of the spectrum. It can be one of the reasons responsible for the nonlinearity of the output power dependences (Fig. 9).

The Bi-doped fiber lasers based on PGSB fibers show a temperature dependence of the output power qualitatively similar to those observed for ASB-based BFLs [13]. For this reason, in all experiments, the fiber was rewound on a high-heat-capacity, temperature-controlled spool providing a good heat contact between the fiber and the spool. This spool was placed into a thermostatted cell. All results described above were obtained at room temperature.

The temperature dependences of the output power of the BFLs based on PGSB fibers were measured in the range (-80 - +80) $^{\circ}$ C. In these experiments we varied the temperature of the active bismuth fiber only. The temperature of all other elements of the laser scheme (Fig. 8) remained constant (+22.5 $^{\circ}$ C).

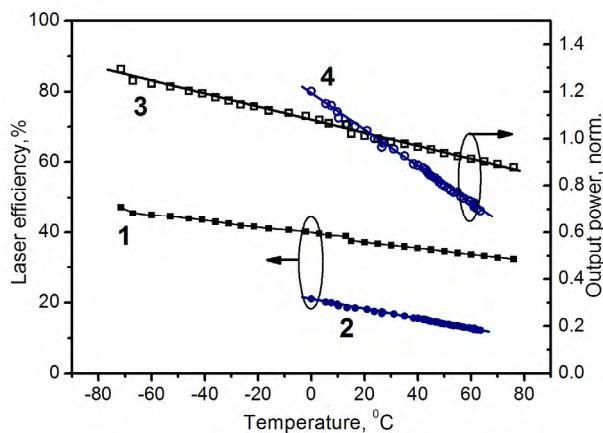


Fig. 11. Variation of the optical-to-optical efficiency of the Bi-doped fiber laser with temperature at the fixed pump power: **1** - PGSB fiber laser L(1330,50), $P_{pl}=14$ W; **2** - ASB fiber laser [13], $\lambda_L=1160$ nm, $P_{pl}=8$ W; Variation of the output laser power of the BFL normalized to unity at room temperature (the pump power is fixed): **3** - PGSB fiber laser L(1330,50), $P_{pl}=14$ W; **4** - ASB fiber laser [13], $\lambda_L=1160$ nm, $P_{pl}=8$ W.

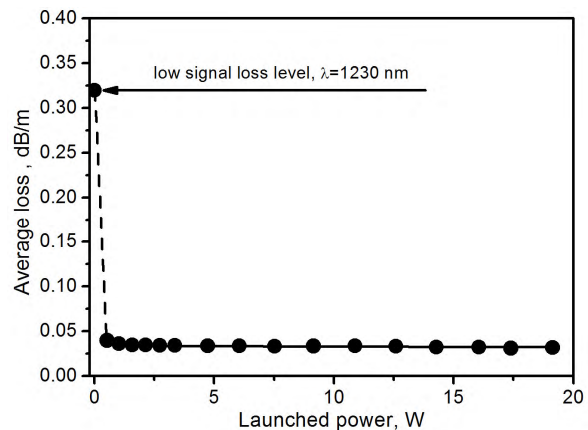


Fig. 12. Average optical losses of the F1 fiber against the launched power at 1230 nm.

One of the measured Bi-fiber laser output power dependences on fiber temperature is shown in Fig. 11. As indicated in this picture, the efficiency of the PGSB fiber laser increased on cooling and went down on heating of the active fiber. Similar dependences for an ASB fiber laser at 1160 nm [13] are also shown in Fig. 11. A comparison of these dependences for PGSB and ASB fibers (Fig. 11, 1 and 2) shows that BFL based on the PGSB fiber demonstrates two times higher efficiency than the ASB fiber based laser in comparable experimental conditions. Nevertheless, the measured temperature dependences are similar to each other qualitatively. We can compare these dependences quantitatively normalizing them to unity with respect to the output power of the lasers, e.g., at room temperature (Fig. 11, lines 3 and 4). In such a case, one can see that the slope of line 3 (PGSB fiber) is $2.8 \cdot 10^{-3} \text{ }^\circ\text{C}^{-1}$, and the slope of line 4 (ASB fiber) is $8 \cdot 10^{-3} \text{ }^\circ\text{C}^{-1}$. So, the considered ASB fiber laser is approximately three times more sensitive to temperature variations than the PGSB fiber laser.

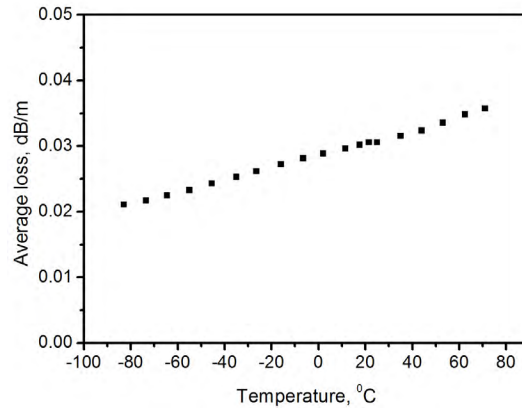


Fig. 13. Temperature dependence of unsaturable optical losses of the F1 fiber at the wavelength of 1230 nm.

The unsaturable absorption of the F1 fiber was measured at the wavelength of pump radiation (1230nm) and the results are shown in Fig. 12. The unsaturable loss is approximately 10 times lower than the low signal level loss (in contrast to the 1/3 ratio of the same values for the ASB fiber investigated in [13]). We believe that the low value of unsaturable losses is an essential contribution to the higher efficiency of the PGSB fiber laser. The observed dependence of the unsaturable optical losses on temperature (Fig. 13) is in a good agreement with the observed temperature dependence of the F1 fiber efficiency.

5.2 Lasers at a wavelength of 1480 nm.

BFLs at the wavelength of 1470 nm based on PGSB fibers demonstrated earlier an efficiency of the order of 3% upon pumping at 1230 nm [6]. The shift of the pump wavelength to the wavelength of 1340 nm (to the region of higher absorption in the F2 fiber, see Fig. 7b) enabled us to increase the efficiency of the laser essentially. For this purpose, a two-cascaded Raman fiber laser based on a phosphosilicate fibers was used. A similar Raman laser with different frequency shifts in each cascade was described in [14].

The wavelength of 1480 nm is far enough (40 nm) from the maximal gain wavelength of the F2 fiber. Nevertheless, lasers L(1480, 50) and L(1480, 3.5) (see Table 1) revealed an efficiency with respect to the pump power launched into the fiber of 21% and a maximal slope efficiency of 25%. The measured dependences of the output power on the absorbed pump power for these lasers are shown in Fig. 14. The dependence for L(1480, 3.5) is nonlinear, similar to the case of BFLs at wavelengths ~1330 nm described above. The slope efficiency of the laser at a low pump power level is essentially lower and is equal to $\approx 9\%$. The maximal output power obtained was 2W.

The optical gain in F2 fiber at the wavelength of 1480 nm turned out to be high enough for lasing with an output mirror reflectivity of 3.5%. However, the efficiency of laser L(1480, 3.5) was somewhat lower (13%). The spectrum of the optical radiation of laser L(1480, 50) is shown in Fig. 15. Except the output radiation of the BFL (Fig. 15, 1), one can see here an essential part of unabsorbed pump power ($\lambda=1340$ nm, Fig. 15, 2). Besides, this figure also shows residues of the pump power of the Raman laser cascades at $\lambda=1268$ nm (Fig. 15, 3) and $\lambda=1085$ nm (Fig. 15, 4).

Taking into account the shape of the F2 fiber gain spectrum (Fig. 7b), it should be expected that lasers based on this fiber can demonstrate an essentially higher efficiency at the wavelengths close to the gain maximum (1440 nm).

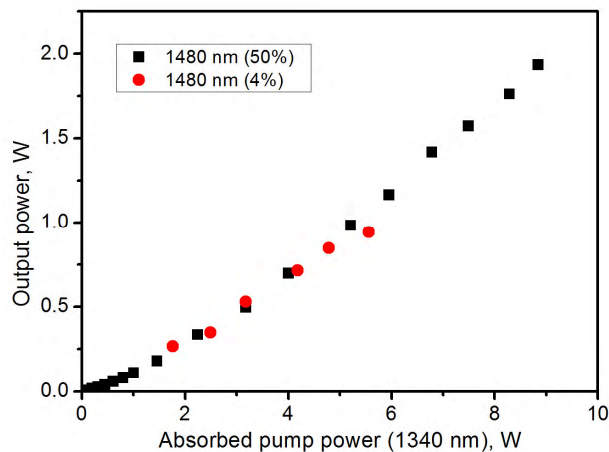


Fig. 14. Variation of the output power with absorbed pump power for Bi-fiber lasers based on the F2 fiber. The lasing wavelength and the OC reflectivity are indicated for each laser.

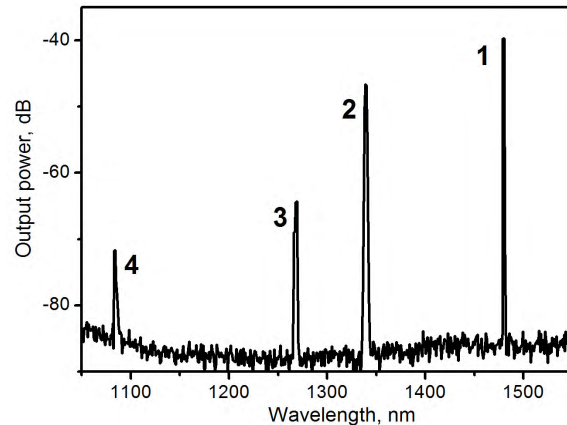


Fig. 15. Spectrum of radiation at the output of laser L(1480, 50).

6. CONCLUSION

Thus, we have demonstrated Bi-doped fiber amplifiers operating in the wavelength regions near 1320 nm and 1440 nm with a maximal gain greater than 20 dB and a noise figure of 4-6 dB at pump powers of the order of 200 mW. As the active medium, Bi-doped phosphogermanosilicate fibers were used. The parameters of these experimental Bi-doped fiber amplifiers are intermediate in gain coefficient between erbium and Raman fiber amplifiers. Besides, watt-level Bi fiber lasers have been demonstrated at 1280, 1330, 1340, 1360, and 1480 nm with the maximum output power of up to 10W and with the efficiency of up to 50% for the first time.

REFERENCES

- 1 Bufetov I.A., Dianov E.M., "Bi-doped fiber lasers", *Laser Physics Letters*, **6**, 487-504 (2009).
- 2 Murata K., Fujimoto Y., Kanabe T., Fujita H., Nakatsuka M., "Bi-doped SiO₂ as a new laser material for an intense laser", *Fusion Engineering and Design*, **44**, 437-439 (1999).
- 3 Dvoyrin V.V., Mashinsky V.M., Dianov E.M., Umnikov A.A., Yashkov M.V., Guryanov A.N., "Absorption, fluorescence and optical amplification in MCVD bismuth-doped silica glass optical fibres" in Proc. European Conference on Optical Communications, Glasgow, September 25-29, 2005, paper Th 3.3.5. (2005).
- 4 Haruna T., Kakui M., Taru T., Ishikawa Sh., Onishi M., "Bismuth-doped silicate glass fiber for ultra-broadband amplification media," in Proc. Optical Amplifiers and Their Applications Topical Meeting, Budapest, August 7-10, 2005, paper MC3.
- 5 Dianov E.M., Firstov S.V., Khopin V.F., Gur'yanov A.N., Bufetov I.A., "Bismuth doped fibre lasers and amplifiers emitting in a spectral region of 1.3 μ m" *Quantum Electron.* **38**(7), 615-617 (2008).
- 6 Bufetov I.A., Firstov S.V., Khopin V.F., Medvedkov O.I., Guryanov A.N., Dianov E.M. "Bi-doped fiber lasers and amplifiers for spectral region of 1300-1470 nm" *Opt. Lett.* **33**, 2227-2229 (2008).
- 7 Fujimoto Y., Nakatsuka M. "Optical amplification in bismuth-doped silica glass", *Applied Physics Letters*, **82**, 3325 (2003).
- 8 Seo Y.-S., Fujimoto Y., Nakatsuka M., "Amplification in a bismuth-doped silica glass at second telecommunication windows", *CLEO 2005*, paper CThR6 (2005).
- 9 Seo Y.-S., Fujimoto Y., Nakatsuka M., "Optical amplification in the 1300nm telecommunications window in a Bi-doped silica fiber", *CLEO 2006*, paper CTu16 (2006).
- 10 Dvoyrin V.V., Mashinsky V.M., Umnikov A.A., Guryanov A.N., Dianov E.M., "Lasers and amplifiers based on telecommunication fibers doped with bismuth", 18th International Laser Physics Workshop (LPHYS'09, July 13 - 17, 2009, Barcelona, Spain), Book of abstracts, p.646 (2009).
- 11 Dianov E.M., Melkumov M.A., Shubin A.V., Firstov S.V., Khopin V.F., Guryanov A.N., Bufetov I.A., "Bismuth-doped fiber amplifier for the wavelength region 1300-1340 nm", *Quantum electronics*, **39**(12), 1099-1101 (2009).
- 12 Desurvire E. *Erbium doped fiber amplifiers*. John Wiley & Sons, Inc., Hoboken, New Jersey, 770p., Chapter 5 (2002).
- 13 Dianov E.M., Shubin A.V., Melkumov M.A., Medvedkov O.I., Bufetov I.A. "High-power cw bismuth-fiber lasers" *JOSA B*, **24**(8), 1749-1755 (2007).
- 14 Dianov E. M., Bufetov I. A., Bubnov M. M., Grekov M. V., Vasiliev S. A., Medvedkov O. I. "Three-cascaded 1407-nm Raman laser based on phosphorus-doped silica fiber", *Opt. Lett.* **25**(6), 402-404 (2000).